Biomedical Optics EXPRESS

Spectral phasor analysis of Pyronin Y labeled RNA microenvironments in living cells

Laura M. Andrews,[1,2] Mark R. Jones,[1] Michelle A. Digman,[2] and Enrico Gratton[2,*]

[1]*University of Western Sydney, School of Science and Health, Richmond, New South Wales, Australia*
[2]*Laboratory for Fluorescence Dynamics (LFD), University of California, Biomedical Engineering Department, Irvine, California 92697-2715, USA*
**egratton@uci.edu*

Abstract: We show that the spectral phasor approach of the fluorescent dye Pyronin Y (PY) can be used to identify specific RNA subspecies of ribonuclear proteins complexes in live cells. We applied spectral phasors to isolate intracellular RNA species with similar spectral properties. We identified at least 4 different PY labeled species in live cells and further spatially mapped their presence at the pixel level. Most notable were transcripts in the nucleoli which were spectrally similar to RNA clusters in the cytoplasm. We propose that these species represent ribosomal RNA and clustered ribonucleoprotein complexes. Further, we observed within this cluster Cajal bodies in the proximity of the nucleolus. In addition, transcripts in the cytoplasm undertook a filamentous morphology composed of multiple puncti structures which individually localized along and close to mitochondria but were distinct from mitochondria.

OCIS codes: (300.0300) Spectroscopy; (300.6280) Spectroscopy, fluorescence and luminescence.

References and links

1. R. R. Cowden and S. K. Curtis, "Supravital experiments with Pyronin Y, a fluorochrome of mitochondria and nucleic acids," Histochemistry **77**(4), 535–542 (1983).
2. Z. Darzynkiewicz and S. P. Carter, "Photosensitizing effects of the tricyclic heteroaromatic cationic dyes pyronin Y and toluidine blue O (tolonium chloride)," Cancer Res. **48**(5), 1295–1299 (1988).
3. Z. Darzynkiewicz, J. Kapuscinski, S. P. Carter, F. A. Schmid, and M. R. Melamed, "Cytostatic and cytotoxic properties of pyronin Y: relation to mitochondrial localization of the dye and its interaction with RNA," Cancer Res. **46**(11), 5760–5766 (1986).
4. F. Traganos, H. A. Crissman, and Z. Darzynkiewicz, "Staining with pyronin Y detects changes in conformation of RNA during mitosis and hyperthermia of CHO cells," Exp. Cell Res. **179**(2), 535–544 (1988).
5. G. Bao, W. J. Rhee, and A. Tsourkas, "Fluorescent probes for live-cell RNA detection," Annu. Rev. Biomed. Eng. **11**(1), 25–47 (2009).
6. M. A. Digman, V. R. Caiolfa, M. Zamai, and E. Gratton, "The phasor approach to fluorescence lifetime imaging analysis," Biophys. J. **94**(2), L14–L16 (2008).
7. C. Stringari, A. Cinquin, O. Cinquin, M. A. Digman, P. J. Donovan, and E. Gratton, "Phasor approach to fluorescence lifetime microscopy distinguishes different metabolic states of germ cells in a live tissue," Proc. Natl. Acad. Sci. U.S.A. **108**(33), 13582–13587 (2011).
8. E. B. van Munster and T. W. Gadella, "Fluorescence lifetime imaging microscopy (FLIM)," Adv. Biochem. Eng. Biotechnol. **95**, 143–175 (2005).
9. B. K. Wright, L. M. Andrews, J. Markham, M. R. Jones, C. Stringari, M. A. Digman, and E. Gratton, "NADH distribution in live progenitor stem cells by phasor-fluorescence lifetime image microscopy," Biophys. J. **103**(1), L7–L9 (2012).
10. F. Fereidouni, A. N. Bader, and H. C. Gerritsen, "Spectral phasor analysis allows rapid and reliable unmixing of fluorescence microscopy spectral images," Opt. Express **20**(12), 12729–12741 (2012).
11. T. Kiss, "Biogenesis of small nuclear RNPs," J. Cell Sci. **117**(25), 5949–5951 (2004).
12. P. J. Santangelo, N. Nitin, and G. Bao, "Live cell imaging of messenger RNA co-localization with mitochondria," in *Proceedings of the 2005 Summer Bioengineering Conference* (2005), pp. 701–702.
13. P. J. Santangelo, N. Nitin, and G. Bao, "Direct visualization of mRNA colocalization with mitochondria in living cells using molecular beacons," J. Biomed. Opt. **10**(4), 044025 (2005).
14. P. J. Santangelo, B. Nix, A. Tsourkas, and G. Bao, "Dual FRET molecular beacons for mRNA detection in living cells," Nucleic Acids Res. **32**(6), e57 (2004).

#174046 - $15.00 USD Received 8 Aug 2012; revised 10 Nov 2012; accepted 19 Nov 2012; published 19 Dec 2012

1. Introduction

The fluorescent probe Pyronin Y (PY) is an environment sensitive probe which has been used to target cell structures including RNA, DNA and organelles. Specifically, PY binds to double stranded RNA (dsRNA) including messenger RNA (mRNA), transfer RNA (tRNA) and ribosomal RNA (rRNA) [1–4]. The aim of this study is to determine whether there are sufficient differences in the spectral properties of PY that can be use to determine which nucleic acid subtype PY is bound in the cell environment. This is of relevance particularly in the cytoplasm and nucleus where multiple RNA subtypes may be present [5] and distinction of these PY labeled species based on intensity only is unfeasible.

In a microscopy fluorescence image of a cell, PY may bind to the various transcript subtypes resulting in the inability to distinguish which RNA the probe is bound to. Overall this means the apparent uniform labeling of cytoplasmic transcripts as well as labeled transcripts in the nucleolus are generically attributed to dsRNA. As a consequence there is no definitive way to identify which species of RNA are positioned where in the cell, or the number of species present in the analysis.

Spectral demixing and principle component analysis (PCA) provide standard means of deconstructing emission profiles. However spectral demixing requires prior knowledge of spectral components and PCA analysis could be problematic in identifying specific components in systems where there is a continuum of states. When a probe is interacting with multiple species, spectral demixing and PCA are deemed impractical due to difficulties associated with obtaining a pure sample to analyze individual probe/transcript interactions. A cuvette analysis of emission profiling of different RNAs with PY is unattainable due to difficulties associated with the extraction and isolation of RNA subtypes where a loss of up to 90% of transcripts can occur [5].

2. Methods

To assess live cell spectral dynamics and properties of PY and to further verify if spectral differences infer the presence of different RNA subtypes with reference to cell organelles, the NIH3T3 cell line was cultured in DMEM supplemented with 10% FBS and PEN/STREP. The cells were maintained in a 37°C, 5% CO_2 incubator and plated onto a 35 mm MatTek dish pre-coated in fibronectin (3 μg/mL) 24 hours prior to imaging. The cells were exposed to PY (12 μM) at the time of plating. Cells were imaged within 5 hours of plating and maintained in a heating stage set to 37°C, 5% CO_2.

All measurements were acquired using the Lambda mode of the Zeiss LSM710 confocal microscope. The excitation wavelength was 514nm (maximum 9% laser power) with a collection bandwidth of 416-728nm. A c-Apochromat 40× 1.20NA Korr M27 water objective was used to acquire images of 256 × 256 size. The pixel dwell time was set to 177.85μs. Images were collected as either an individual lambda scan with the collection of 32 channels combined to create one image or as a stack of images (32 channels each image) with different focal planes (~1μm step size) where each individual image was globally analyzed. At 514nm excitation, cell autofluorescence was insignificant.

3. Results and discussion

To assess if small spectral changes in a single microscopy image, with reference to PY, may provide information on the number of different transcripts in a live sample each image was spectrally decoded and the average emission profile produced (Fig. 1). The color coded emission profiles corresponded to one acquired plane of focus. With each plane, small emission profile shifts were observed which appears to be indicative of the quantity of detected species and the type of detected transcript.

#174046 - $15.00 USD Received 8 Aug 2012; revised 10 Nov 2012; accepted 19 Nov 2012; published 19 Dec 2012

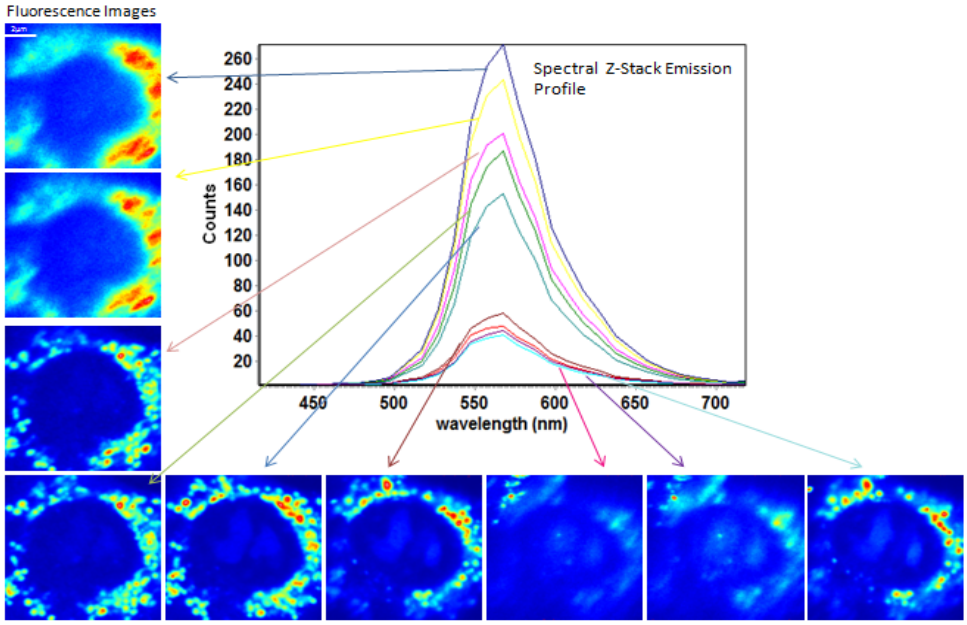

Fig. 1. Z-stack intensity images and corresponding image averaged emission profiles of PY labeled species in a live NIH3T3 cell. The color coded arrows link each emission spectrum with the corresponding plane of focus. Small spectral shifts were observed for each plane.

To assess if the observed small spectral shifts could be used to determine different RNA species associated with different cell organelles (nuclear, cytoplasmic and nucleolar), we used a method which does not require prior spectral knowledge of individual PY/RNA subtype interactions. Instead, our method is based on the correlation between spectral components and the spatial distribution of the probe where specific spatial features can be identified in images and associated with spectral features.

Demixing techniques include traditional spectral demixing but also the phasor plot technique in FLIM (fluorescence lifetime imaging). The use of phasors enables the identification of the molecular environment of a probe [6–9]. The use of the spectral component in the traditional application of the phasor plot was first proposed by Fereidouni et al in 2012 as a means of unmixing multiple spectra in an image [10]. In order to be used for unmixing this method, as originally proposed, requires prior knowledge of each component contributing to the emission profile or the individual spectra could be inferred from spectral phasor plot if they are sufficiently separated.

Instead, our approach to spectral phasors does not require prior knowledge of spectral components even if the phasor positions are not well separated. In the spectral phasor technique, each pixel in the image is used to construct a spectral profile which is Fourier transformed to produce two co-ordinates for each pixel in the spectral phasor plot as described in [10]. This provides a graphical representation of each spectrum where each experimental data point is represented in the coordinates of the spectral phasor plot without demixing. Clusters of points in the phasor plot simply correspond to species with similar spectra. Since different clusters can be selected by a computer algorithm, we can recognize if a specific cluster corresponds to identifiable spatial features even if the clusters are in part superimposed. It is this correlation (if it exists) between spatial features and clusters of points in the phasor plot that will allow us to identify the spectral signature of specific features of the image.

In the spectral phasor plot, each wavelength maps to a different phase (smaller angles are blue emission and larger angles are red emission). The phase can be identified with the center of mass of the spectral emission. The modulus (radius of the pixel in the phasor plot) depends

#174046 - $15.00 USD Received 8 Aug 2012; revised 10 Nov 2012; accepted 19 Nov 2012; published 19 Dec 2012

on the average width of the spectrum of each fluorescent component [10]. Alterations in the phase and modulus of the spectral phasor may highlight differences between each emission profile at a pixel level. An increase in the phase infers a shift towards a longer wavelength while a decrease in the spectral profile width results in an increase in the modulus.

Each emission profile will usually appear as a single or multiple spatially distinguishable clusters where a cluster refers to aggregates of pixels of the same or similar emission profile within the spectral phasor plot. Manual selection of the clusters results in the selection of these emission profiles within the image as each pixel in the phasor plot corresponds to a pixel of the image. The image can however be used as a spatial reference where clusters may be selected based on the structural characteristics of the cell. For example, selection of nucleoli compartments in the image selects clusters in the nucleolus as well as any other pixels of similar emission profile if within the same cursor confinement region.

Overall this process enables the number of fluorescent species and contribution of the species to be determined by an assessment of both the linear combination of the species, and morphology (width) of the clusters, without the requirement for spectral unmixing or prior knowledge of the spectra of each individual labeled component. The use of spectral phasors selection through the correlation with image features provided a means to select for spectral components based on the structural and morphological characteristics of the fluorescent sample without bias. The 32 channel lambda stack images (Figs. 2A and 3A) were put into the SimFCS software for spectral phasor analysis (available from http://www.lfd.uci.edu/). In these images intensity differences are apparent with the most intense PY labeled transcripts within the cytoplasm followed by the nucleolus. The spectral phasor analysis was carried out for each cell and plotted in the phasor plot. The spectral phasor of PY in DMEM, DMEM alone and background were determined. Background displayed minimal variance from the 0 point of reference inferring minimal spectral contribution (flat spectrum) (Fig. 2C: left). The intensity of the PY in solution (used at 5× the cell concentration to induce fluorescence in solution) resulted in a single compact pixel cluster. PY in solution at a cell concentration did not fluorescence as significantly and thereby did not contribute to the position of phasor clusters in the cell measurements. Clusters within the phasor plot for cells were selected manually and identified with the presence of PY labeled species in different cell regions or organelles.

#174046 - $15.00 USD Received 8 Aug 2012; revised 10 Nov 2012; accepted 19 Nov 2012; published 19 Dec 2012

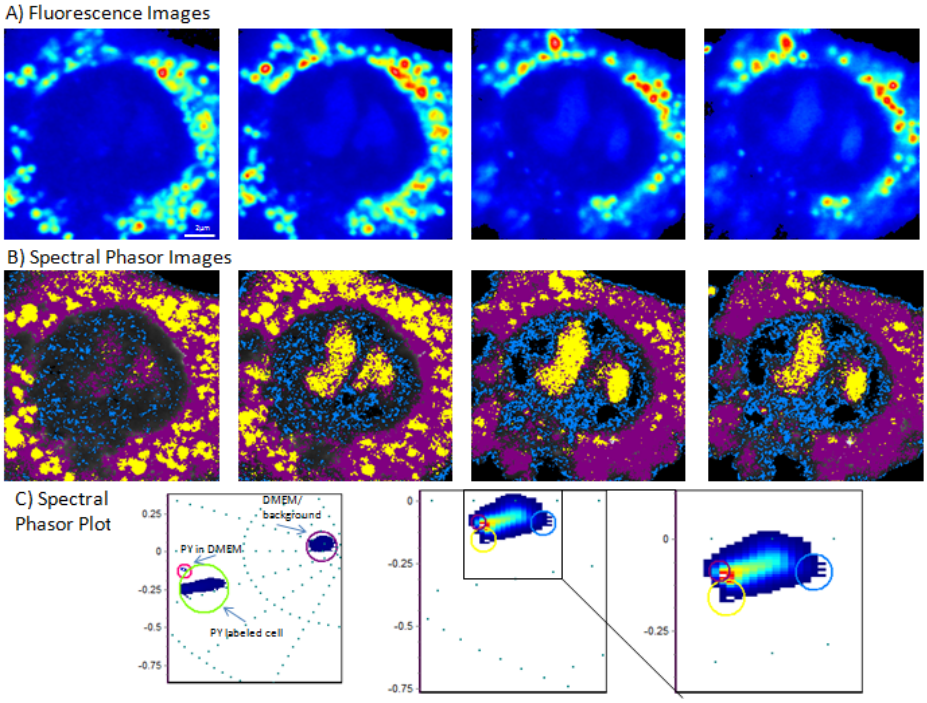

Fig. 2. Fluorescence intensity (A) and spectral phasor z-stack images (B) of PY labeled species in a live NIH3T3 cell with cluster selection through the use of three cursors (radius = 3-5 nm) in the distribution plot (C: centre and magnified right). Cluster selection provided three main species. One selection (yellow painted) mainly in the nucleoli and sporadically in the cytoplasm may be associated with rRNA and mRNP complexes. The second selection (purple) was positioned throughout the cytoplasm. Species in the nucleus (blue color) appeared positioned around the nuclear periphery or surrounding the nucleoli and represented a linear combination of PY transcripts and background. Cluster distributions were also globally assessed for PY in DMEM and DMEM/background. Background displayed minimal migration from the centre of the distribution plot with DMEM inducing deviation from 0 as pictured (C: left). PY in solution displayed a compact cluster at an average wavelength of 557.7 ± 1.5nm width 37.1 ± 0.7nm positioned slightly below 0 line of reference (C: left).

In Fig. 2 we identified three distinct PY labeled species with reference to structural components which displayed different wavelength maxima and widths. The most apparent species distinction was within the nucleolus: wavelength 559.6 ± 2.9nm width 31.6 ± 1.4nm. Interestingly, cluster selection of the nucleoli transcripts also lead to isolation of regions in the cytoplasm. We propose these clusters consist mainly of rRNA within the nucleoli (Fig. 2B yellow nucleoli) and messenger ribonucleoprotein (mRNP) complexes (Fig. 2B yellow cytoplasm) which in each instance displayed similar spectral properties.

We further identified labeled species in the cytoplasm of each cell which displayed two structural forms; a filamentous form composed of short puncti structures or individual clusters. The detected species in the cytoplasm had an average wavelength of 555.2 ± 1.7nm and width 30.2 ± 1.0nm. These species appeared to decorate and at times be detected also within the nucleoli (Fig. 3B). We believe the involvement of PY labeled ribosomes in the cytoplasm result in slight elongation if the ribosomes. We further suggest the second species in the nucleolus (Figs. 2B and 3B: purple) may be ribosomes undergoing assembly. The nuclear components were characterized by a spectral average of 554.8 ± 1.7nm and width 36.3 ± 3.1nm. All of the determined average spectra center of mass ranged at less than 4.8nm apart, inferring spectral phasor is able to spectrally separate multiple fluorescent species below 5nm.

#174046 - $15.00 USD Received 8 Aug 2012; revised 10 Nov 2012; accepted 19 Nov 2012; published 19 Dec 2012

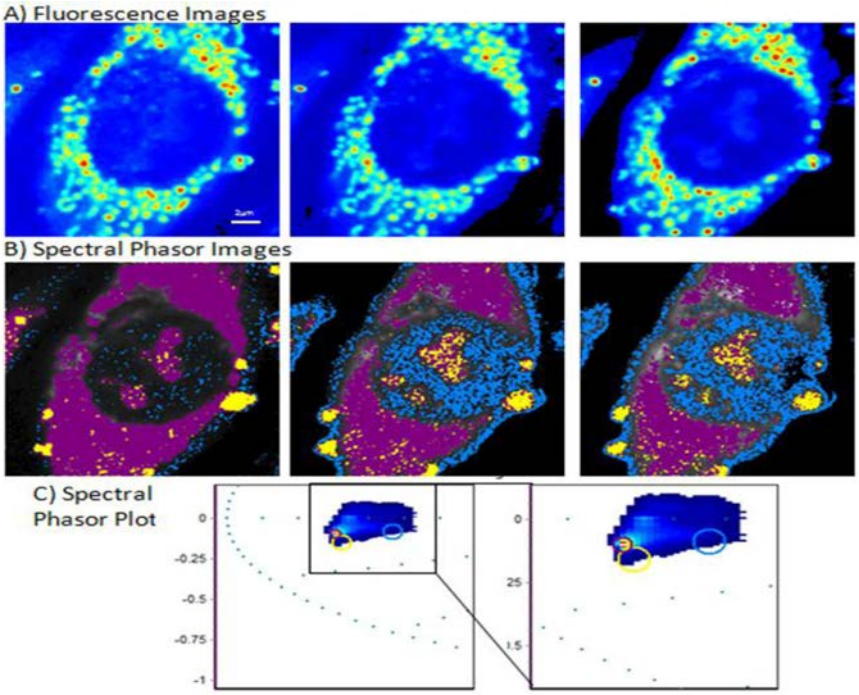

Fig. 3. Fluorescence intensity (A) and spectral phasor z-stack images (B) of PY labeled species in a live NIH3T3 cell with cluster selection through the use of three cursors with a maximum radii of 4nm within the distribution plot (C: left and magnified: right). Cluster selection again provided three main species.

Interestingly the cytoplasmic transcripts appeared to, at times (Fig. 3), coat the nucleolus and be positioned within it suggesting these species may be ribosomes positioned in the cytoplasm or being assembled in the nucleolus.

Spectral phasor analysis showed the same components in most cells (N>20) and over the days. However some cells displayed an additional PY labeled species within the nucleus. This was often seen in structures in close proximity or interacting with the nucleolus (data not shown) suggesting the labeling of Cajal bodies (Fig. 4) due to this interaction and the comparable size [11].

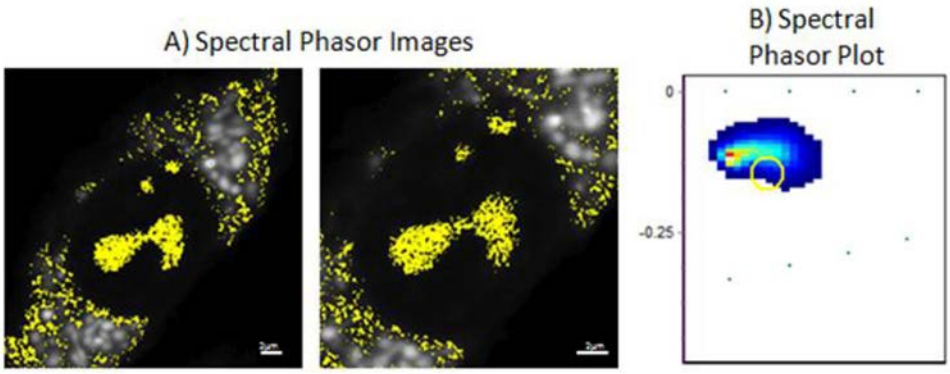

Fig. 4. Spectral phasor images (A) and spectral phasor plot (B) of PY labeled species in a live NIH3T3 cell. The two images display the same plane of focus but two different zooms. Cluster selection occurred through the use of a single cursor with a radius of 3nm. The PY selected for with the yellow cluster (lower images) displayed similar properties to the other cells however there were small detected clusters within the nucleus which bear similar characteristics to Cajal bodies (number present, size and morphology).

#174046 - $15.00 USD Received 8 Aug 2012; revised 10 Nov 2012; accepted 19 Nov 2012; published 19 Dec 2012

To assess the interaction of the monitored transcripts with cell structures in the cytoplasm, we labeled mitochondria with mito-eGFP. The PY labeled short puncti structures of the cytoplasmic transcripts were seen to move along the same tracks as the mitochondria (Fig. 5) confirming the interaction of RNA with the mitochondrial matrix [5,12–14]. However, we found very little co-localization of the green labeled mitochondria and red labeled RNA species.

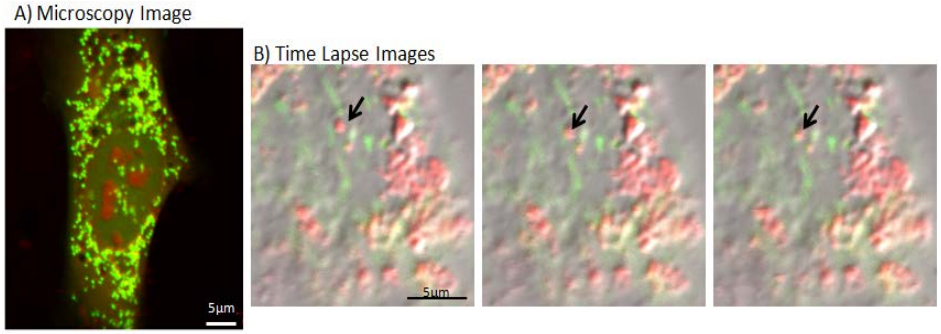

Fig. 5. Fluorescence microscopy image (A) of live NIH3T3 cells dual labeled with mito-eGFP (green) and PY (red) 512 × 512 image size. The time lapse images (B) show the spatial position of the transcripts (red) with the mitochondrial matrix (green). Note the mobilization of the transcripts which appear to move along single mitochondria (black arrows) as a function of time (6 second intervals).

4. Conclusions

This application of spectral phasors provides a means by which many different bound components, using a single probe, may be spectrally distinguished and selected for within an image even if spectral similarities place their wavelengths less than 5nm apart. It furthermore provides a promising technique to differentiate between RNA subtypes based on spectral emission patterns. To our knowledge, this is the first time that PY is shown to have a range of spectral properties within cells expressing different RNA-riboprotein complexes. The universal labeling of RNA's with PY could complement specific species labeling and allow an assessment of overall RNA abundance and location in the cytoplasm and in the nucleus.

Acknowledgments

This work is supported in part by NIH grants NIH-P41-RR03155 and P41 GM103540 (EG, MD) and NIH P50-GM076516 (EG).

#174046 - $15.00 USD Received 8 Aug 2012; revised 10 Nov 2012; accepted 19 Nov 2012; published 19 Dec 2012